The United Nations University

GEOTHERMAL TRAINING PROGRAMME
Orkustofnun, Grensásvegur 9,
IS-108 Reykjavík, Iceland

Reports 1997
Number 10

1-D INTERPRETATION OF MAGNETOTELLURIC DATA FROM SOUTHERN LEYTE GEOTHERMAL PROJECT, PHILIPPINES

Carlos Emmanuel F. Los Baños
Geothermal Division, Geoscientific Dept.,
PNOC-Energy Development Corporation,
PNPC Complex, Merritt Road, Ft. Bonifacio,
Makati City, Metro Manila,
PHILIPPINES

ABSTRACT

A magnetotelluric (MT) survey consisting of 39 soundings, was conducted at the Southern Leyte geothermal project from January to April 1997. 1-D interpretation of the data shows two low-resistivity zones persisting down to depths of about 3000 m, one on the west, and a broader one northeast of Mt. Cabalian. A resistive zone is delineated beneath Mts. Cabalian and Cantodoc.

1. Introduction

The Southern Leyte geothermal project (SLGP), formerly known as the Mt. Cabalian geothermal prospect covers the geothermal area on the southern tip of the island of Leyte (Figure 1). It has been the target of exploratory work since 1983. In 1997, between January and April, a magnetotelluric (MT) survey was conducted there to probe the resistivity signature of the area at deep levels and to augment the existing data obtained from earlier surveys. The aim of the survey was to reassess the geothermal potential of the area. A total of 39 soundings were measured using a Phoenix V-5 MT system, applying the remote reference method.

2. Previous studies

Geoscientific studies have been carried out by the Philippine National Oil Company Energy Development Corporation (PNOC-EDC) in Southern Leyte since 1983 to assess the area's geothermal potential. These studies include detailed geological mapping, geochemical sampling and geophysical surveys consisting of Schlumberger resistivity traversing (SRT), vertical electrical sounding (VES) and regional gravity methods. The results of these surveys are discussed briefly.

2.1 Geology

The geothermal area is located on the island of Leyte, west of the Philippine Trench where the Philippine

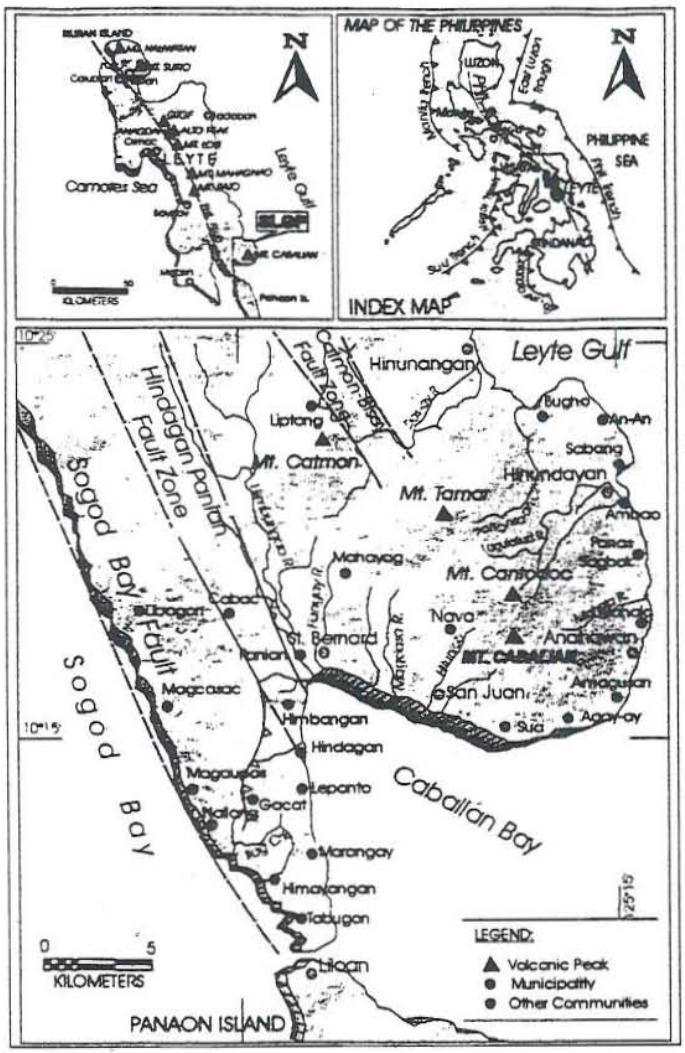

FIGURE 1: Map showing the location of the Southern Leyte geothermal project (Leynes et al., 1996)

Plate is subducting in a southwestward direction (Figure 1). Mt. Cabalian, is part of the eastern Philippine volcanic front which includes Mts. Bato, Mahagnao and Lobi (Datuin, 1982).

The geology of Southern Leyte is shown in Figure 2 (Leynes et al., 1996). The lithology is classified into 5 major stratigraphic units. The Cretaceous ultramafics (CU) is the oldest rock unit mapped in the area. Exposures of this unit, comprised of dark green to green, highly fractured serpentinites, are found in the southwest near the Cabalian Bay. This unit is overlain unconformably by buff to cream-colored and fossiliferous Tertiary limestones (TL) on the southwest. Exposed in the western and northeastern portions of the area are sequences of clastic sedimentary rocks of conglomerates, turbidites, sandstones and calcisiltites capped by thin but massive coral limestone deposits collectively referred to as the Tertiary clastics (TC). Late Tertiary volcanic rocks (TV) are found in the north and western sectors of Mt. Cabalian and are composed of moderately to highly altered basaltic andesite to andesite lava flows, as well as tuffs and tuff breccias intruded by microdiorite dikes. The Quaternary volcanics (QV) include the small strato-volcanoes such as Mts. Cantodoc and Cabalian, which are comprised of alternating sequences of pyroclastic and lavas.

The main structures mapped in the area include two major splays of the Philippine fault, the Hindagan-Panian and Catmon-Bisay faults, delineated west and north-northwest of the study area. Several minor faults were also mapped in the area (Figures 1 and 2).

2.2 Geochemistry of thermal areas

Most of the thermal features found in Southern Leyte, such as hot and warm springs, are located on the eastern and western flanks of Mt. Cabalian (Figure 2). A unique thermal feature is the presence of "kaipohans" or patches of ground characterized by intense acid alteration and high concentrations of gases such as CO_2 and H_2S. In general, the spring waters are classified into 3 groups:

1. Acid condensate, composed mostly of dissolved gases like H_2S, i.e Ilaya;
2. Mixed Cl-HCO_3-SO_4, indicating significant deep hydrothermal components, i.e. Mainit, Mahalo and Tabun;
3. Pre-dominantly HCO, i.e. Nava, Hitunlob and Hugpa.

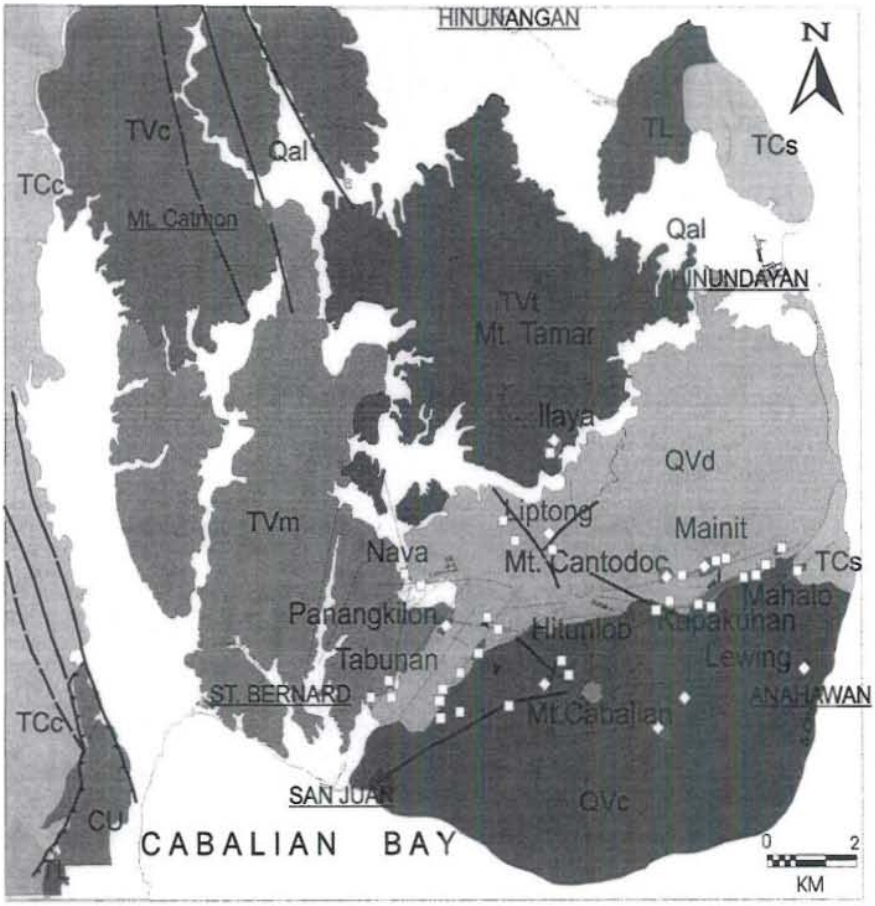

FIGURE 2: Geologic map of the Southern Leyte geothermal project (Leynes et al., 1996), CU - Cretac. ultramafics; TL - Tertiary limest..; TC - Tertiary clastics (c - conglomer., s - sandst.); TV - Tert. volc.(c - Mt. Catmon, t - Mt. Tamar); QV - Quat. volc.(d - Mt. Cantodic, c - Mt. Cablian); Qal - Quaternary alluvium, the squares and diamonds represent the thermal areas

Analysis and plotting of these waters in a Na-K-Mg ternary diagram (Figure 3) reveal that all water samples group near the immature water region, forming a single dilution line which points to a source fluid temperature of 240°C. This also suggests that the thermal springs come from a single hydrothermal system (Leynes et al., 1996).

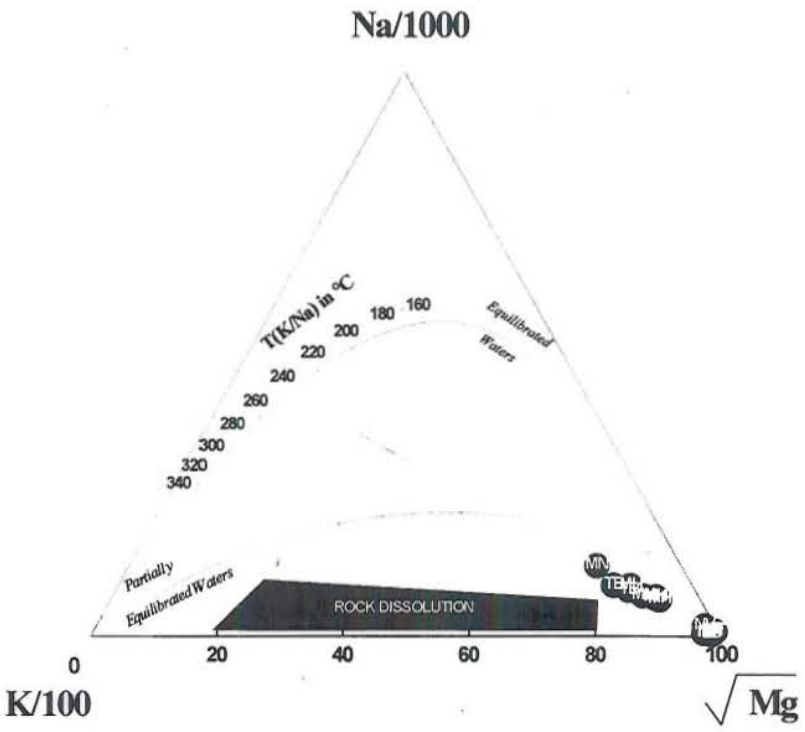

FIGURE 3: Na-K-Mg ternary plot of waters from Southern Leyte (Leynes et al., 1996), circles show samples from geothermal areas

2.3 Geophysics

Resistivity surveys such as the DC Schlumberger resistivity traverse and vertical electrical sounding methods with a maximum AB/2 spacing of 1000 m, were conducted in

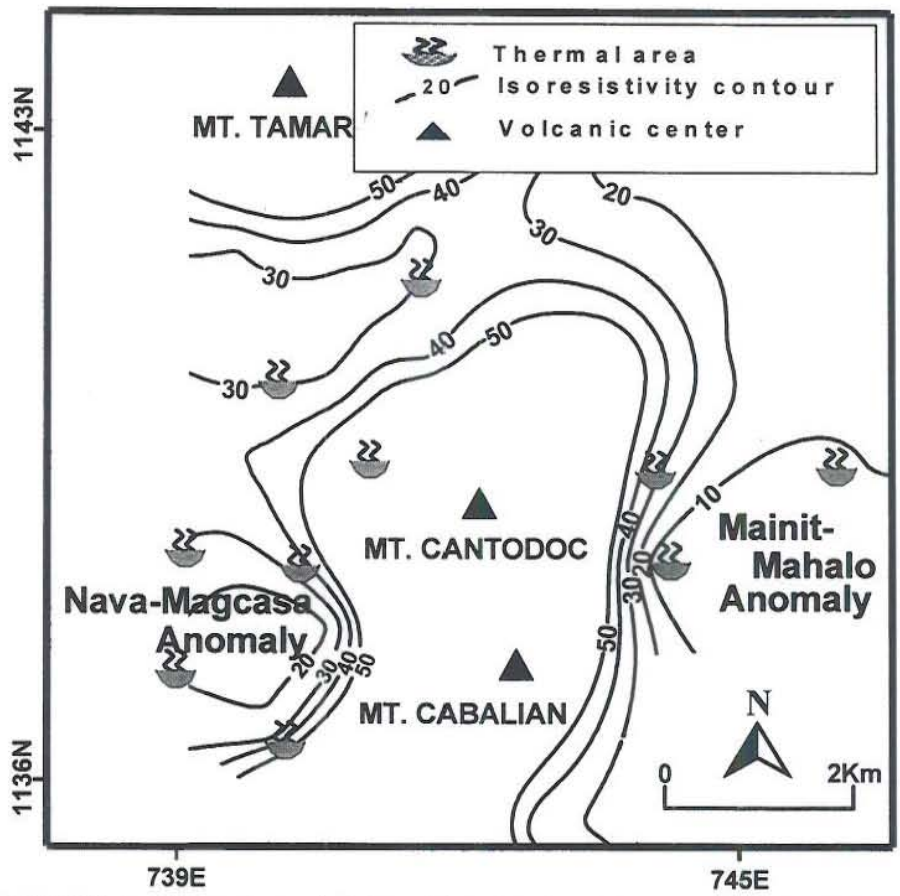

FIGURE 4: Apparent resistivity of the Southern Leyte geothermal project at about 1000 m depth (Tebar et al., 1989)

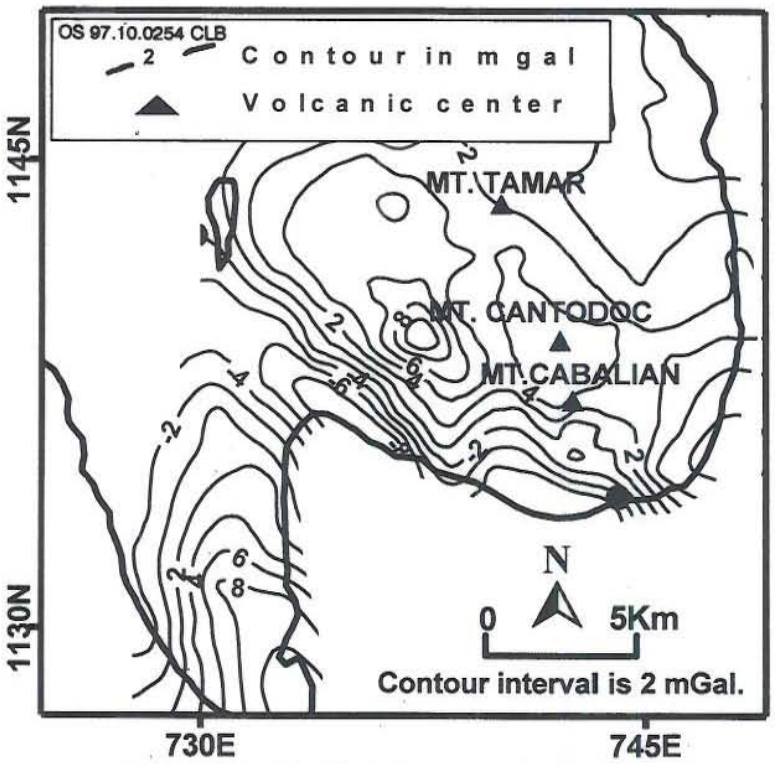

FIGURE 5: Residual Bouger anomaly map of Southern Leyte (Catane and Apuada, 1996)

Southern Leyte as early as 1989 (Tebar et al., 1989). The resistivity surveys delineated two low-resistivity zones (<20 Ωm) situated on the eastern (Mainit-Mahalo) and west-southwestern (Nava-Magcasa) flanks of Mt. Cabalian (Figure 4). These low-resisitivity zones are separated by a zone of relatively high resistivity beneath Mt.Cabalian. The low-resistivity anomalies were postulated to be the outflow zones of the geothermal system in the region. The upflow zone is inferred to be beneath Mt. Cabalian. A gravity survey was then carried out in 1996. The regional gravity survey revealed two gravity highs located directly beneath and northwest of Mt. Cabalian (Figure 5) modelled to be shallow intrusives and interpreted to be the heat source of the geothermal system (Catane and Apuada, 1996).

3. BASIC THEORY OF MT

The magnetotelluric (MT) method is a remote sensing technique which measures the natural electromagnetic fields from which it is possible to model the earth's resistivity structure. Natural sources for MT signals are lightning activity during thunderstorms for frequencies above 1 Hz and micropulsations in the magnetosphere caused by solar activity, for frequencies below 1 Hz.

3.1 The relationship between the electrical and the magnetic fields

For a vertically incident plane wave and a homogenous earth, Maxwell's equation reduces to

$$\frac{\partial E_y}{\partial z} = i\omega\mu H_x \tag{1}$$

$$\frac{\partial H_x}{\partial z} = (\sigma + i\omega\varepsilon)E_y \tag{2}$$

$$\frac{\partial E_x}{\partial z} = -i\omega\mu\ H_y \tag{3}$$

$$\frac{\partial H_y}{\partial Z} = -(\sigma + i\omega\varepsilon)E_x \tag{4}$$

where

E_x, E_y	are the electrical field in the x and y directions;
H_x, H_y	are the magnetic field in the x and y directions;
σ	is the conductivity in S/m;
ω	$= 2\pi f$, is the angular frequency, f is the frequency in Hz;
μ	is the magnetic permeability in H/m;
ε	is the electrical permittivity in C^2/Nm^2;
i	$=\sqrt{-1}$.

From Equations 1 and 2, and 3 and 4, we get respectively

$$\frac{\partial^2 E_x}{\partial z^2} = k^2 Ex \tag{5}$$

$$\frac{\partial^2 E_y}{\partial z^2} = k^2 E_y \tag{6}$$

where

$k^2 = i\,\omega\,\mu\,(\sigma + i\,\omega\,\varepsilon)$.

The general solution to Equations 5 and 6 is

$$E_{x,y} = (A_{x,y}e^{kz} + B_{x,y}e^{-kz}) \tag{7}$$

where A_x, A_y, B_x and B_y are constants.

Since $E_{x,y} \to 0$ as $z \to \infty$, $A_{xy} = 0$, from Equations 1 and 3, we have for the magnetic field

$$H_x = -B_y \frac{k}{i\omega\mu} e^{-kz} \tag{8}$$

$$H_y = B_x \frac{k}{i\omega\mu} e^{-kz} \tag{9}$$

The impedance is defined as the ratio of the orthogonal electric and magnetic fields, i.e

$$Z_{xy} = \frac{E_x}{H_y} = \frac{i\omega\mu}{k} \tag{10}$$

$$Z_{yx} = \frac{E_y}{H_x} = \frac{-i\omega\mu}{k} \tag{11}$$

In the earth, σ is on the order of $1\text{-}10^{-4}$ S/m, $\varepsilon \ll 10^{-7}$, and ω is $10^{-3}\text{-}10^{3}$ Hz; thus $\sigma \gg \omega\,\varepsilon$ and therefore $k^2 \approx i\,\omega\mu\sigma$. Thus, Equations 10 and 11 become

$$Z_{xy} = \frac{i\omega\mu}{\sqrt{i\omega\mu\sigma}} = \sqrt{\frac{\omega\mu}{\sigma}} e^{i\pi/4} \tag{12}$$

$$Z_{yx} = -\sqrt{\frac{\omega\mu}{\sigma}} e^{i\pi/4} = \sqrt{\frac{\omega\mu}{\sigma}} e^{-i3\pi/4} \tag{13}$$

Thus, the specific resistivity of the earth can be calculated according to

$$\rho = \frac{1}{\sigma} = \frac{1}{\omega\mu}|Z_{xy}|^2 = \frac{1}{\omega\mu}|Z_{yx}|^2 \tag{14}$$

In practical units, where E is in mV/m and $B = \mu H$ in nT (gamma), we have

$$\rho = 0.2T|Z_{xy}| = 0.2T|Z_{yx}| \quad (15)$$

where T is the period in s.

For a non-homogeneous earth, we can write in general

$$E_x = Z_{xx}H_x + Z_{xy}H_y \quad (16)$$

$$E_y = Z_{yx}H_x + Z_{yy}H_y \quad (17)$$

or in matrix notation

$$\overline{E} = \overline{Z}\,\overline{H} \quad (18)$$

where Z is the impedance tensor,

and

$$H_z = T_xH_x + T_yH_y \quad (19)$$

where T is called the tipper.

3.2 Skin depth

The depth of penetration of the MT method is given by the concept of skin depth (δ), which is the depth where the strength of the electromagnetic fields has been reduced to e^{-1} from the surface values, or

$$\delta = \left(\frac{2}{\omega\mu\sigma}\right)^{1/2} \quad (20)$$

where

δ	is the skin depth in m;
μ	is the magnetic permeability in H/m;
ω	$= 2\pi f$, is the angular frequency, f is the frequency in Hz;
σ	is the conductivity in S/m.

In simpler form

$$\delta \approx 500\sqrt{\rho T}\ m \quad (21)$$

where T is the period of the signal.

As can be seen from Equations 18 and 19, the low frequencies (i.e. the long periods) penetrates deeper into the earth than high frequencies.

3.3 Non-homogeneous earth

For a one dimensional (1-D) earth (i.e. layered earth) we have the following relationship between the elements of the impedance tensor and the tipper.

$$Z_{xx} = Z_{yy} = 0 \tag{22}$$

$$Z_{xy} = -Z_{xy} \tag{23}$$

$$T_x = T_y = 0 \tag{24}$$

For a two-dimensional (2-D) earth, it is possible to rotate the coordinate system through an angle θ in the horizontal plane, such that

$$Z_{xx} = Z_{yy} = 0 \tag{25}$$

$$Z_{xy} \neq Z_{yx} \tag{26}$$

$$T_x \neq 0,\ T_y = 0 \tag{27}$$

The angle θ is called the principal direction.

For a three-dimensional (3-D) earth, we have, regardless of rotation,

$$Z_{xx} \neq Z_{yy} \neq 0 \tag{28}$$

$$Z_{xy} \neq Z_{yx} \tag{29}$$

$$T_x \neq T_y \neq 0 \tag{30}$$

3.4 Rotation of the impedance tensor

In general, the resistivity structure is three-dimensional. However, it is often possible to approximate the response function (impedance tensor) by 1-D or 2-D cases. If the character of the impedance tensor approximates the 1-D case, we define a new impedance which is invariant to rotation, namely

$$Z_{\text{det}} = \det(Z) = \sqrt{Z_{xx}Z_{xy} - Z_{xy}Z_{yx}} \tag{31}$$

or

$$Z_{ave} = (Z_{xy} - Z_{yx})/2 \tag{32}$$

From these, we define new apparent resistivities and phases

$$\rho_{det} = 0.2T|Z_{det}|^2 \; ; \quad \theta_{det} = arg(Z_{det}) \tag{33}$$

or

$$\rho_{ave} = 0.2T|Z_{ave}|^2 \; ; \quad \theta_{ave} = arg(Z_{ave}) \tag{34}$$

In another case where the impedance shows a 2-D characteristic, the principal direction is found by maximizing $|Z_{xy}(\theta)|^2 + |Z_{yx}(\theta)|^2$ (or equivalently, minimizing $|Z_{xx}|^2 + |Z_{yy}|^2$). This is done by setting $\delta F(\theta)/\delta\theta = 0$, where

$$F = |Z_{xy}(\theta)|^2 + |Z_{yx}(\theta)|^2 \tag{35}$$

which gives

$$\tan 4\theta = \frac{[(Z_{xx} - Z_{yy})(Z_{xy} + Z_{yx})^* + (Z_{xx} - Z_{yy})^*(Z_{xy} + Z_{yx})]}{|Z_{xx} - Z_{yy}|^2 - |Z_{xy} - Z_{yx}|^2} \tag{36}$$

where * is the complex conjugate. The solution for θ is known as Swift's angle (Swift, 1967).

As can be seen from Equation 34, there is a 90° ambiguity with the principal direction, i.e. the direction of the 2-D strike could either be θ or $\theta + 90°$. Choosing the correct one depends on the other available data, either from the horizontal magnetic field or from geological information.

As stated earlier, in a 2-D environment, it is possible to rotate the tipper function T, through an angle ϕ, such that $T_x(\phi) \neq 0$, but $T_y(\phi) = 0$. The rotation that maximizes T_x gives the direction of the 2-D strike direction. Thus, it should be equal to θ or $\theta + 90°$.

3.5 Skewness

The impedance *skew* is defined by

$$skew = \frac{|Z_{xx} + Z_{yy}|}{|Z_{xy} - Z_{yx}|} \tag{37}$$

The *skew* is invariant to rotation and is zero in noise-free 1-D and 2-D cases. It is a useful parameter that describes the three dimensionality of the data.

3.6 Induction vectors

The real (R) and imaginary (I) induction vectors are defined as (Gough and Ingham, 1983)

$$|R| = (T_{x(r)}{}^2 + T_{y(r)}{}^2)^{1/2} \; ; \; \Theta_R = -\tan^{-1}\frac{T_{x(r)}}{T_{y(r)}} \tag{38}$$

$$|I| = (T_{x(i)}{}^2 + T_{y(i)}{}^2)^{1/2} \; ; \; \Theta_I = \tan^{-1}\frac{T_{x(i)}}{T_{y(i)}} \tag{39}$$

where $T\,x,y\,(r)$ and $T\,x,y\,(i)$ are the real and imaginary parts of the tipper. The real induction vector points to deep seated conducting anomalies whereas the imaginary induction arrows point to shallower conductors (Patra and Mallick, 1980).

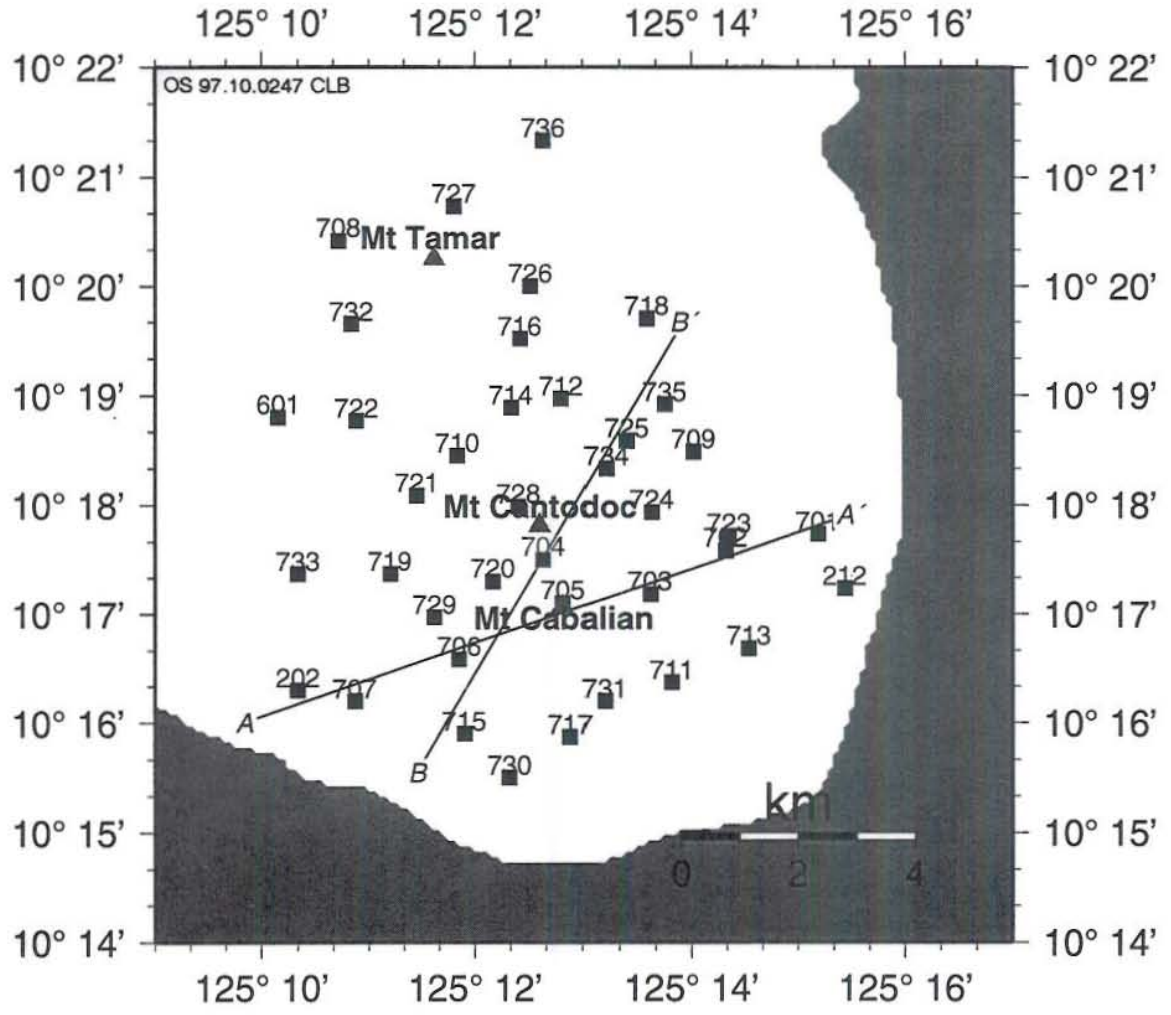

FIGURE 6: Location map of the MT stations, lines A-A' and B-B' show the locations of resistivity cross-sections

4. RESULTS

4.1 Data analysis

For the Southern Leyte geothermal project a total of 39 MT stations (Figure 6) were measured using a Phoenix V-5 MT system which is capable of measuring frequencies in the range of 0.00055 to 384 Hz (Graham, 1991). Stations were spaced about 500 m to 1 km apart. All stations were oriented towards the magnetic north unless the ruggedness of the terrain did not permit it. The remote reference (RR) technique was applied during data acquisition for most sites.

In general, the quality of the MT data acquired was good for periods less than 1 s. Most signals at periods greater than 1 s show scattering and large error bars. The determinant apparent resistivity and phase, which are invariant to rotation were used during the 1-D inversion of the data. The impedance skews for most stations were low (<0.1), indicating little three-dimensionality for the area. Rotation to the principal direction points to an angle of about N135°E, which is consistent to the strike of the major faults found in the area (e.g. Catmon-Bisay fault zone). All the data can bee seen in the appendix, which is published separately (see Los Baños, 1997).

4.2 Induction vectors

Several plots using the real and imaginary components of the induction vectors were made to identify regions of high conductivity in the area. At a period of 0.2 s (Figure 7), the induction arrows are small

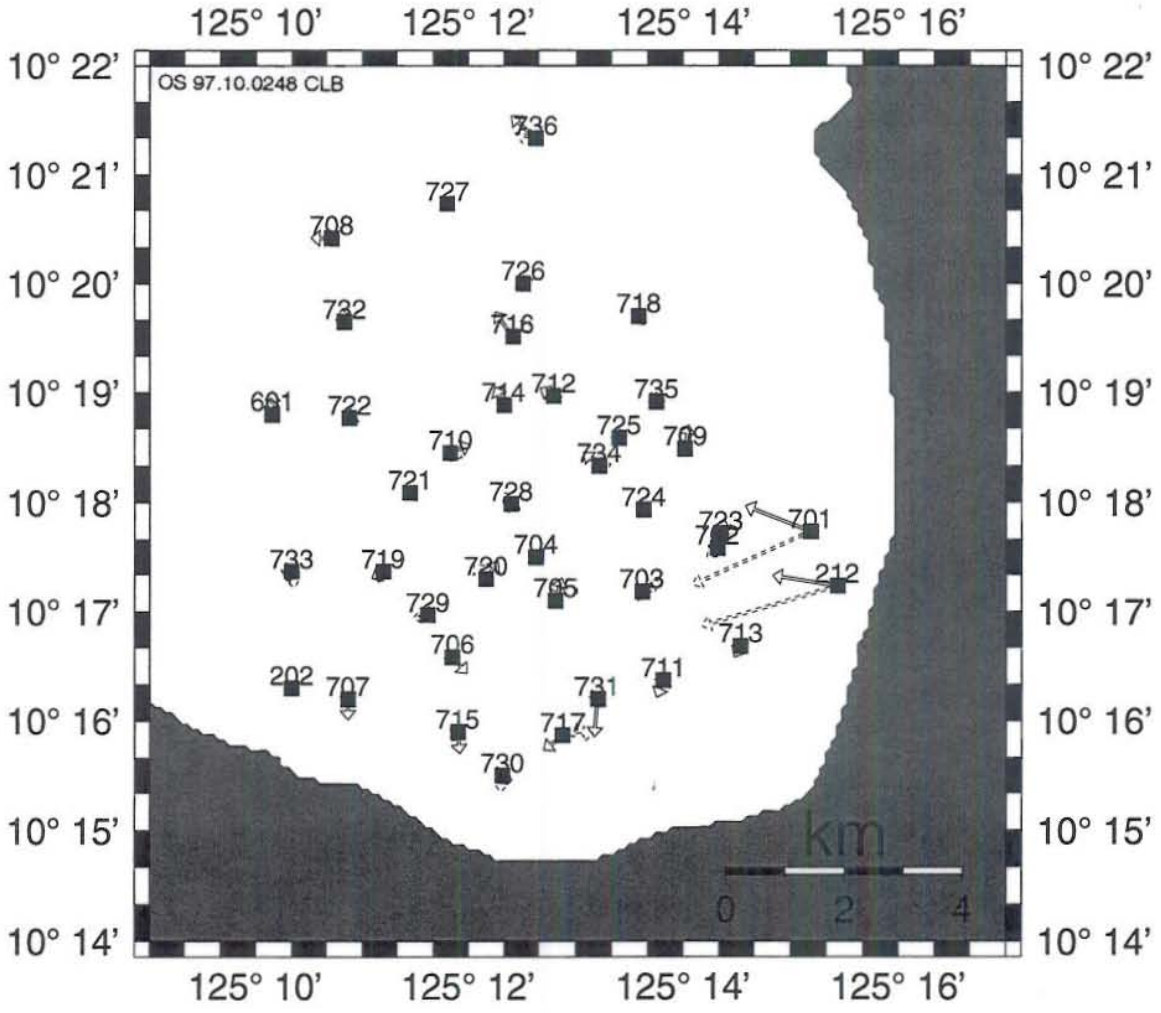

FIGURE 7: Induction vectors at 0.2 s, real vectors shown by solid arrows, imaginary by dashed

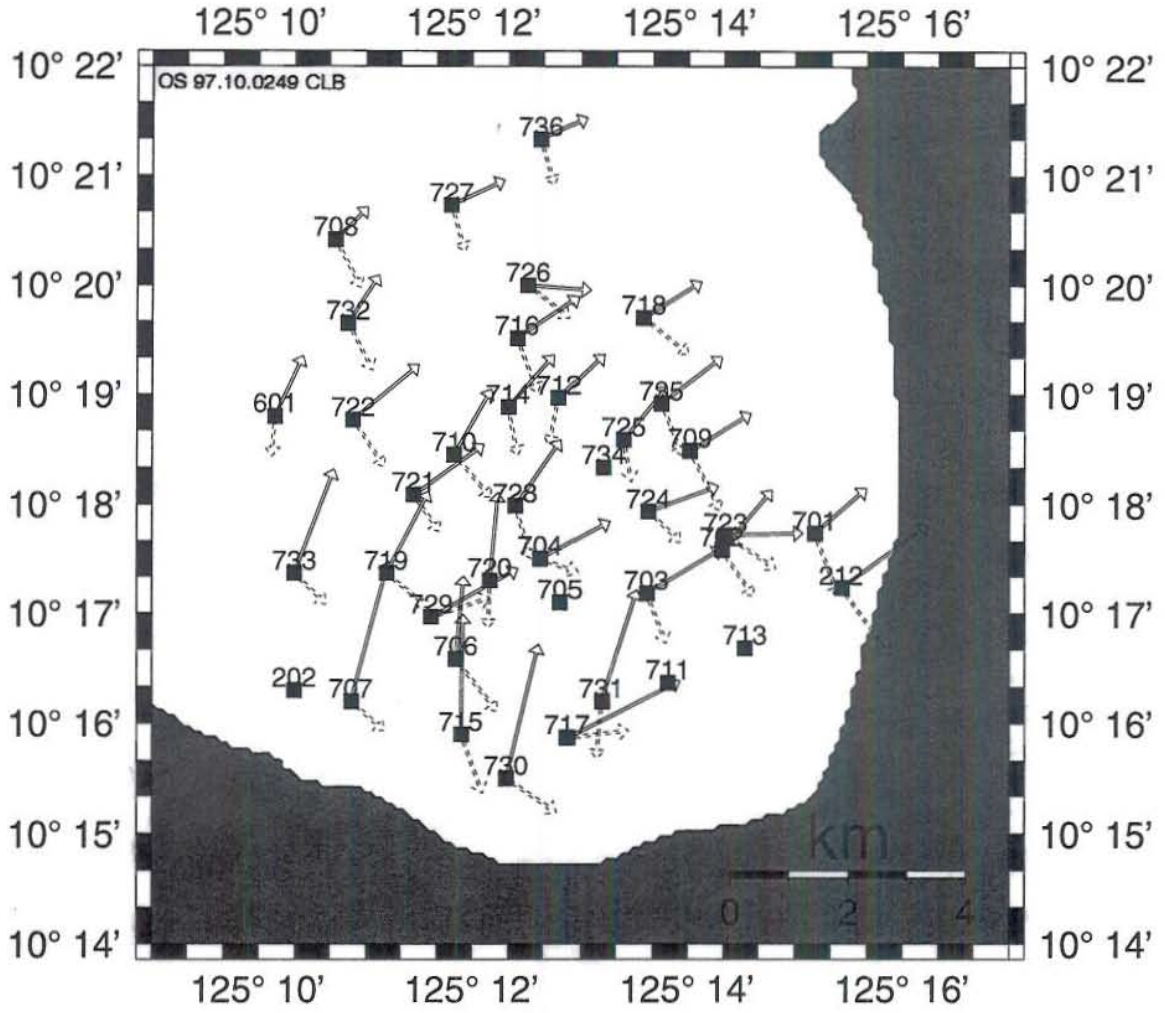

FIGURE 8: Induction vectors at 42.7 s, real vectors show by solid arrows, imaginary with dashed

and inconsistent. The southernmost stations have arrows pointing towards the coast, indicating coastal effect. At a period of 42.7 s (Figure 8), the real induction vectors point to the presence of a deep conductive body in the northeast while the imaginary induction vectors point toward the south-southeast indicating a shallow conductive body in that direction.

4.3 Inversion models

For each MT site in Southern Leyte two inversions were performed, first, with as few layers as possible (hereafter called 1-D layered models), and secondly by Occam inversion, which fits the data to a "smooth" resistivity model. The Occam inversion not only minimizes the difference between the data and the model response but also minimizes the "roughness" (or maximizes the smoothness) of the model. There is a trade off between the model fit to the data and the roughness of the model, i.e. best fit to data gives rough models (Constable et al., 1987). The 1-D layered and Occam models for each MT site can be found in the Appendix (Los Baños, 1997).

The general characteristic of the models from the 1-D inversion show high surface resistivity, then low resistivity (<10 Ωm) at 100 to 2000 m depth, then increasing resistivity with depth.

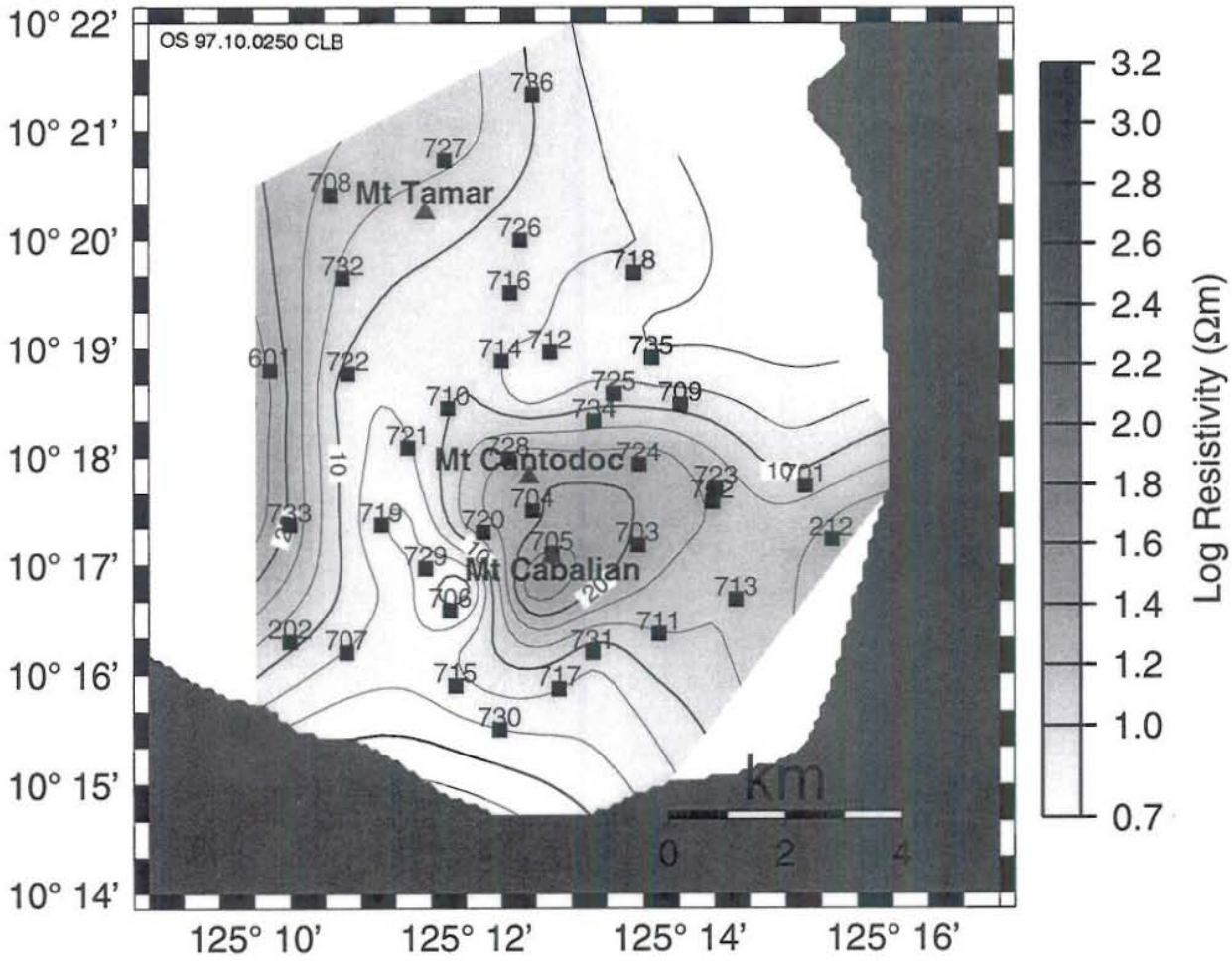

FIGURE 9: Isoresistivity map of the Southern Leyte geothermal project at 300 m depth b.s.l., the contour interval is 0.1 log resistivity in Ωm, light shades show low resistivity and dark shades high resistivity

4.4 Isoresistivity maps

The results of the smooth 1-D Occam data inversion were contoured to make isoresistivity maps at different depths.

The resistivity at 300 m depth below sea level (b.s.l.) in the survey area (Figure 9) is less than 10 Ωm except for the area around Mts. Cabalian and Cantodoc, which is characterized by relatively high resisitivity values >10 Ωm. At 1000 m depth b.s.l. (Figure 10), the broad low-resistivity (< 10 Ωm) anomaly is now separated into two, one in the northeast and the other in the south part of Mt. Cabalian. The area bounded by Mts. Cabalian and Cantodoc is enclosed by higher resistivity values (>20 Ωm). This high-resistivity region extends further to the west. However, it should be noted that the quality of the low-frequency part of the data for sites near Mts. Cabalian and Cantodoc is poor and, therefore, the results not very reliable. At 2000 m depth b.s.l. (Figure 11), the low-resistivity anomaly in the northeast still exists, while the one in the south is greatly reduced and is shifted towards the western portion of Mt. Cabalian. The region beneath Mts. Cabalian and Cantodoc is still characterized by high resistivity values (>20 Ωm). At 5000 m depth b.s.l. (Figure 12) the study area is bounded by resistivity values >50 Ωm except for the anomaly zone in the northeast, where the resistivity is less than 20 Ωm.

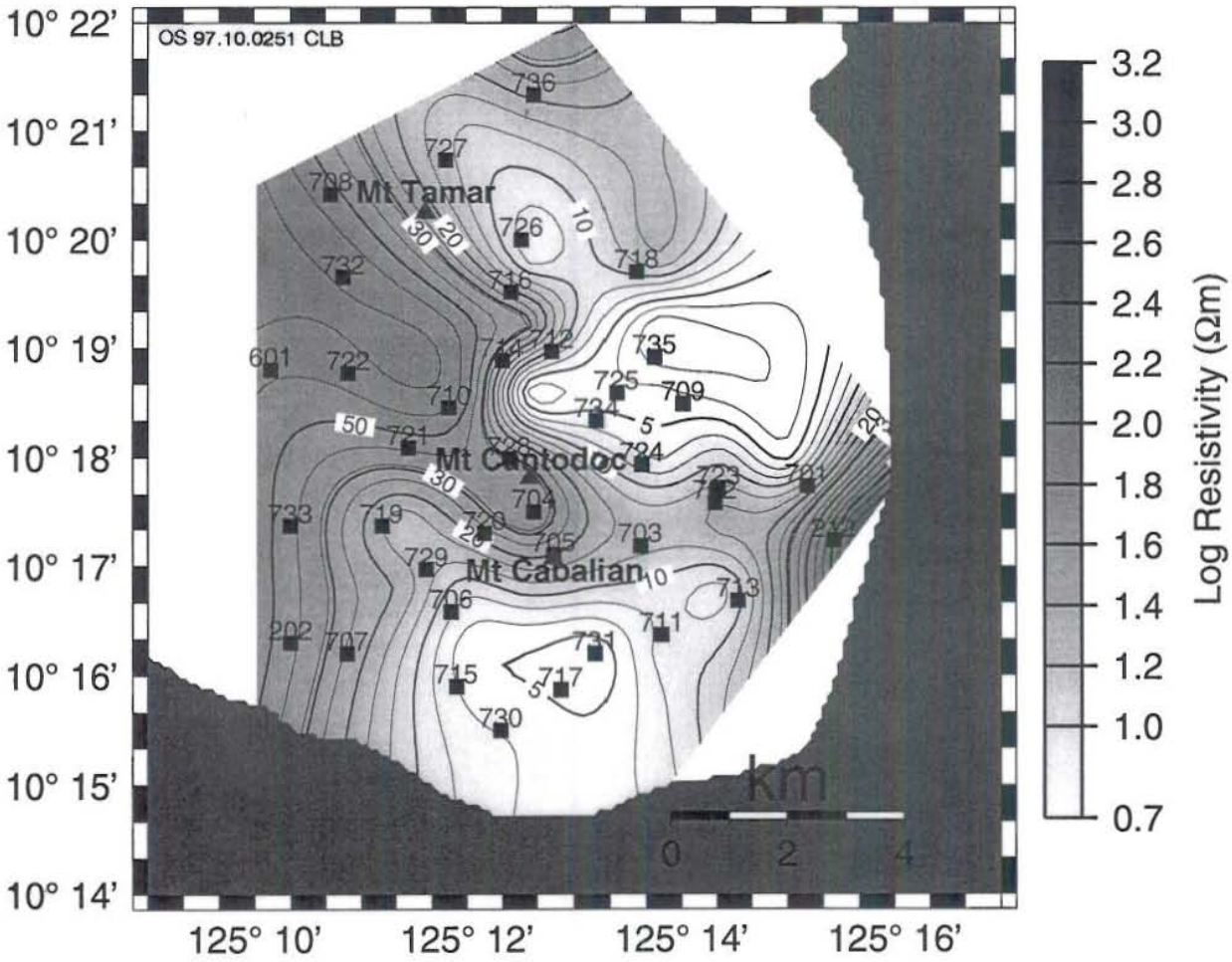

FIGURE 10: Isoresistivity map of the Southern Leyte geothermal project at 1000 m depth b.s.l. the contour interval is 0.1 log resistivity in Ωm, light shades show low resistivity and dark shades high resistivity

4.5 Resistivity cross-sections

Figure 13 shows the resistivity cross-section along line A-A′ (Figure 6), according to the Occam inversion results. The profile runs WSW-ENE. A thin (~150 m) conductive zone is found at about 300 m depth, along the whole cross-section except beneath the southwestern-most station (202). Below is a broad less conductive region down to about 2500 m b.s.l. with resistivity of 10-20 Ωm, except in the northeast where lower resistivity is seen at around 1000-1500 m b.s.l. At greater depths, the resistivity increases. One conspicuous feature is the presence of a high-resistivity zone (>20 Ωm) directly below Mt. Cabalian at 500 to 1000 m depth b.s.l..

A simplified cross-section along AA′ is shown on Figure 14 based on the 1-D layered inversion. It shows the same features, high resistivity at surface, a shallow conductive layer at depths of about 100 to 500 m and a broader conductive layer below it, which gets deeper towards the east. Further below, the resistivity increases with depth. Furthermore, this profile indicate that static shift is not a serious problem for this line. The broad low-resistivity region at 1000-1500 m depth in the northeast which appeared in the Occam inversion (Figure 13) appears as a lower resistivity in the second layer beneath site 701.

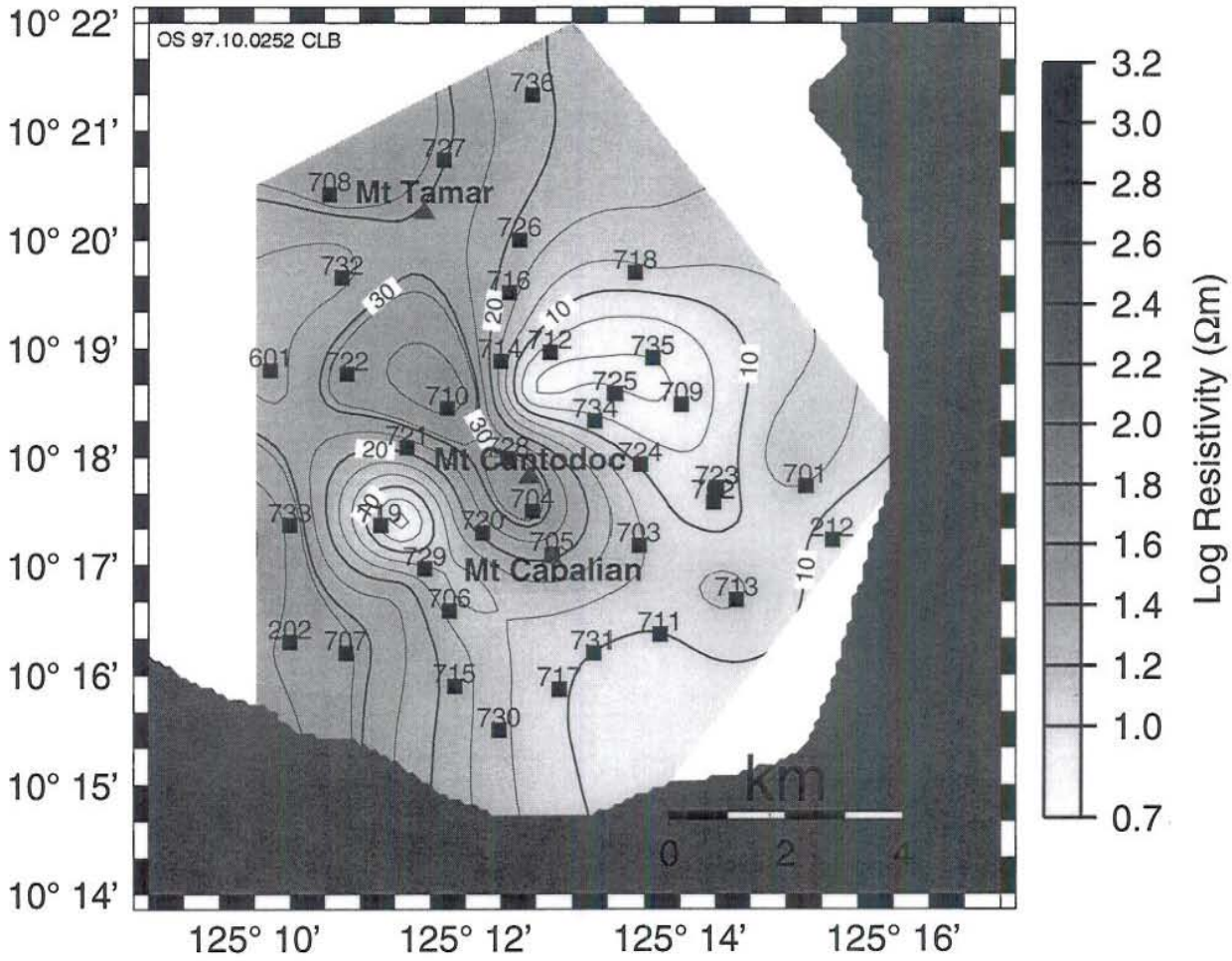

FIGURE 11: Isoresistivity map of the Southern Leyte geothermal project at 2000 m depth b.s.l., the contour interval is 0.1 log resistivity in Ωm, light shades show low resistivity and dark shades high resistivity

Figure 15 shows the results of the Occam inversion along line B-B′ traversing Mts. Cabalian and Cantodoc from southwest to northeast (Figure 6). It shows a high-resistivity layer (>50 Ωm) from the surface down to depths of about 100 m. Three low-resistivity regions are noted. One in the southwest at about 300-1000 m depth b.s.l. with resistivity less than 5 Ωm. The second is in the northern part also at 300-500 m depth b.s.l. with a resistivity less than 5 Ωm and the third below it, at 1000-2500 m depth b.s.l. also with resistivity less than 5 Ωm. A block of relatively high resistivity is detected below the volcanoes starting at a depth of 500 m.

Similar resistivity structures are found by the 1-D layered inversion, shown in Figure 16. A resistive cap rock exists from the surface down to 200 m depth. This is underlain by one to three conductive layers (<12 Ωm) down to about 2000 m b.s.l. In the southwest, the resistivity is <10 Ωm in the first low-resistivity layer down to 500 to 1500 m b.s.l. and becomes shallower towards Mt. Cabalian. Below is a 12-16 Ωm layer down to depths of 2000 m b.s.l., where the resistivity increases again. In the northeastern part, three low- resistivity layers are detected. The first is a thin and highly conductive (<5 Ωm) layer at 100-200 m b.s.l. The second conductor has slightly higher resistivity (10 Ωm) than the first conductor and is found at 200 to 500 m b.s.l. This layer extends to the southwest. The third conductor has a resistivity <5 Ωm at 500 to 2000 m b.s.l. Below, the resistivity increases. Beneath Mts. Cabalian and Cantodoc there is a relatively high resistivity starting at depths of 500 m b.s.l.

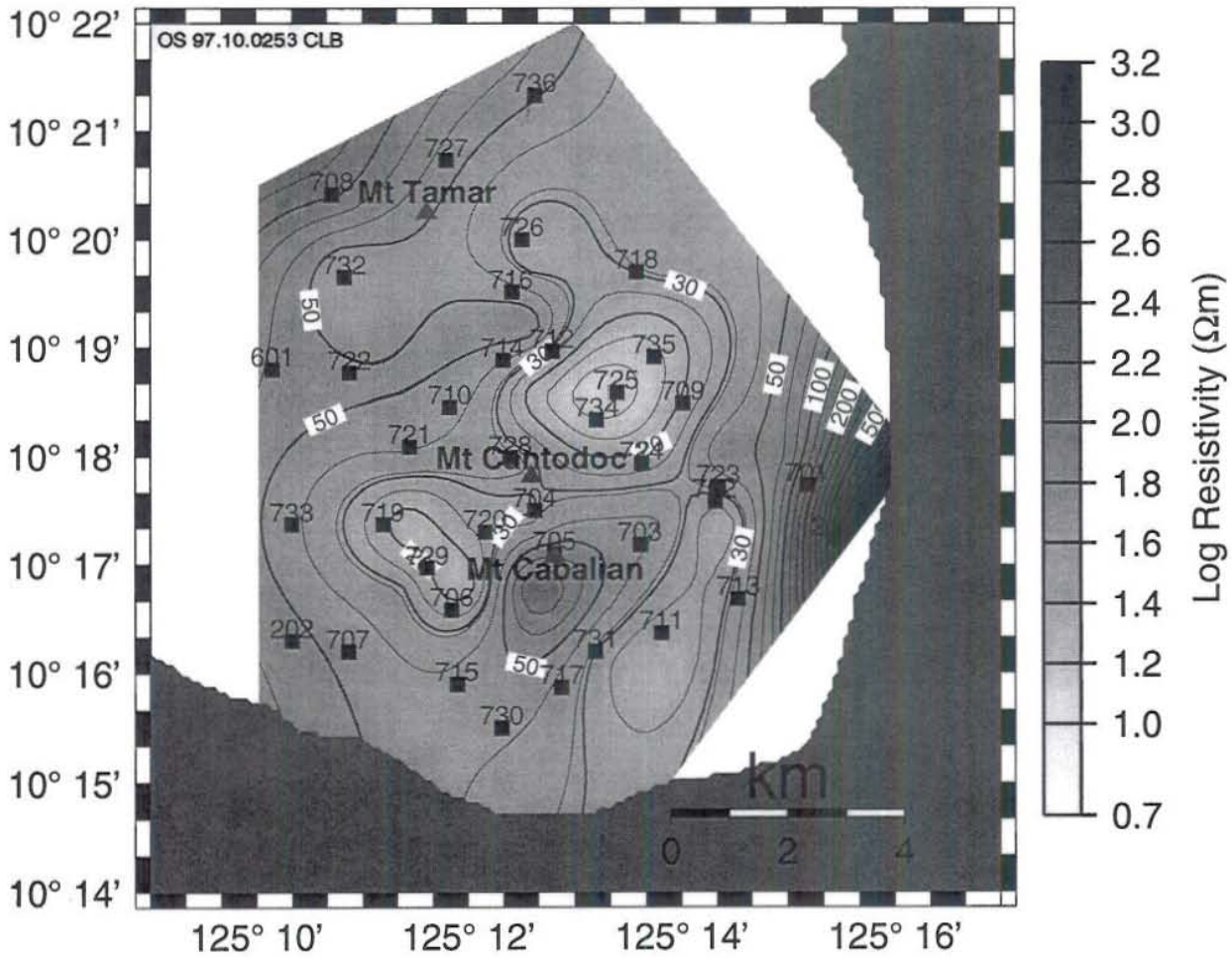

FIGURE 12: Isoresistivity map of the Southern Leyte geothermal project at 3000 m depth b.s.l., the contour interval is 0.1 log resistivity in Ωm, light shades show low resistivity and dark shades high resistivity

5. CONCLUSIONS

The MT survey in Southern Leyte mapped two important low-resistivity anomalies. One is located west-southwest of Mt. Cabalian and the other to the northeast of the same volcano. Similar low-resistivity anomalies had been mapped by DC Schlumberger surveys but their depth extent was not delineated due to the shallow penetration depth of the method. The anomaly on the northeastern side extends deeper (as great as 3000 m) than the southwestern anomaly and is more conductive. The location of this anomaly is indicated by the induction vectors for high periods. The area is capped by a resistive layer that can be associated to the young volcanic deposits of the Quaternary volcanoes Mts. Cabalian and Cantodoc. A localized high-resistivity zone occurs beneath the volcanoes, which can be correlated to the shallow intrusive body modelled by the gravity survey. Highly resistive layers are seen at greater depths.

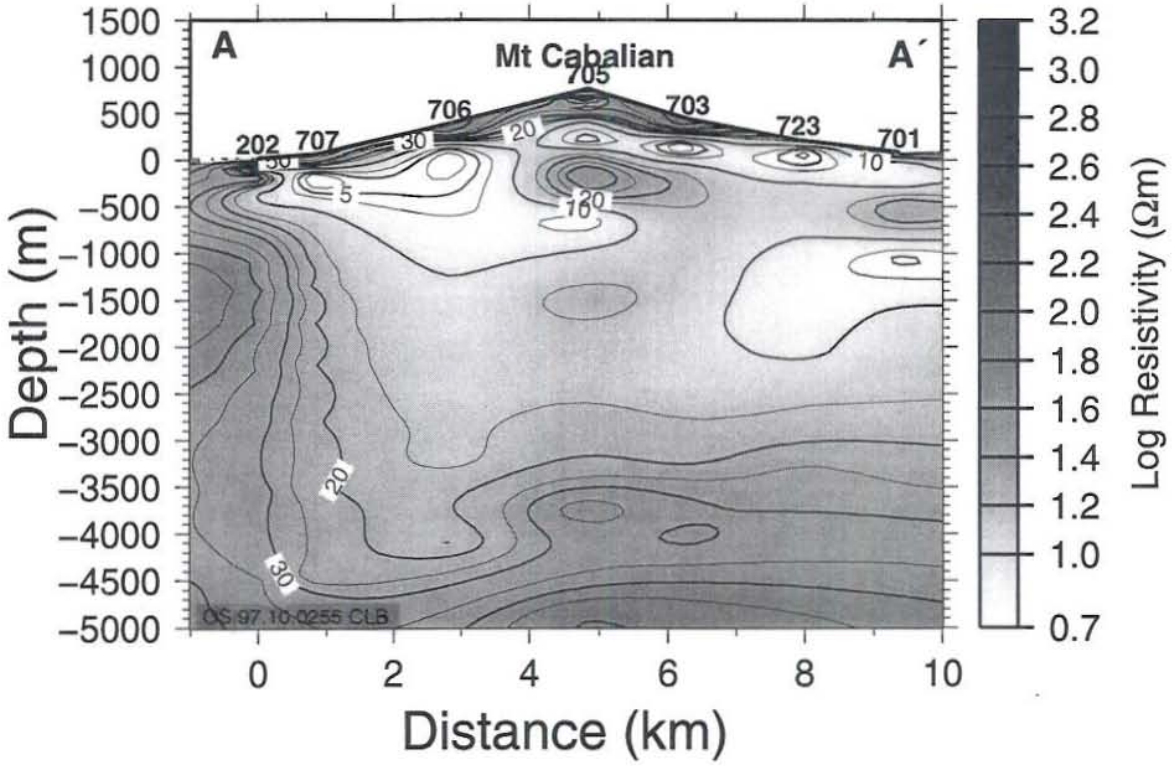

FIGURE 13: 1-D Occam model along cross-section A-A', contour interval is 0.1 log resistivity in Ωm

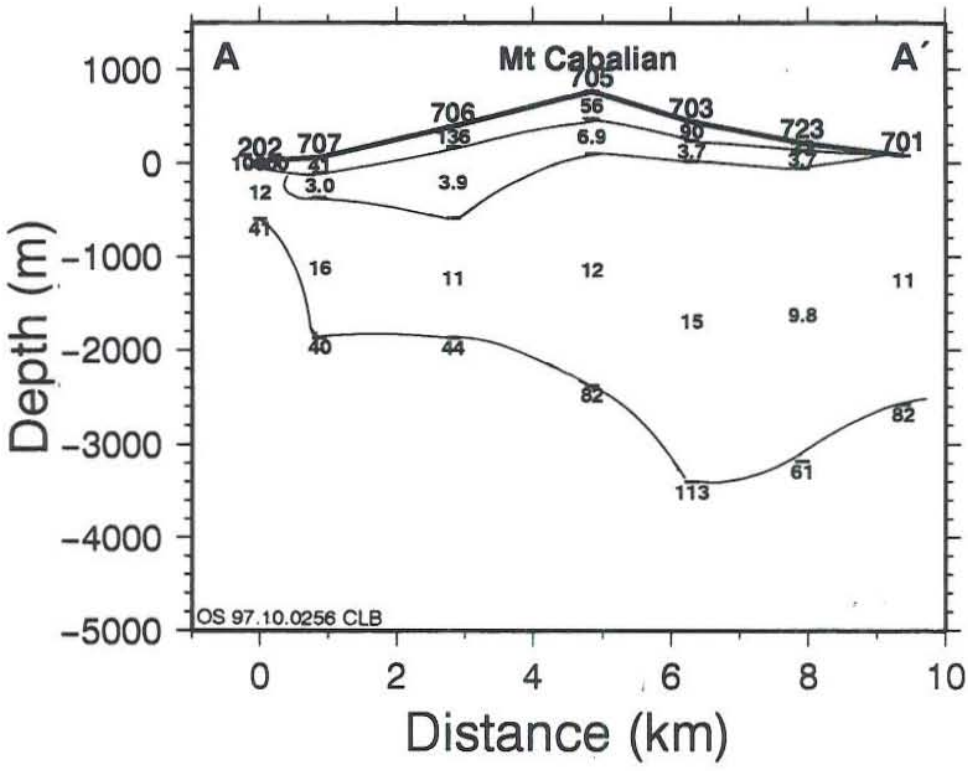

FIGURE 14: 1-D layered model along cross-section A-A', contour interval is 0.1 log resistivity in Ωm

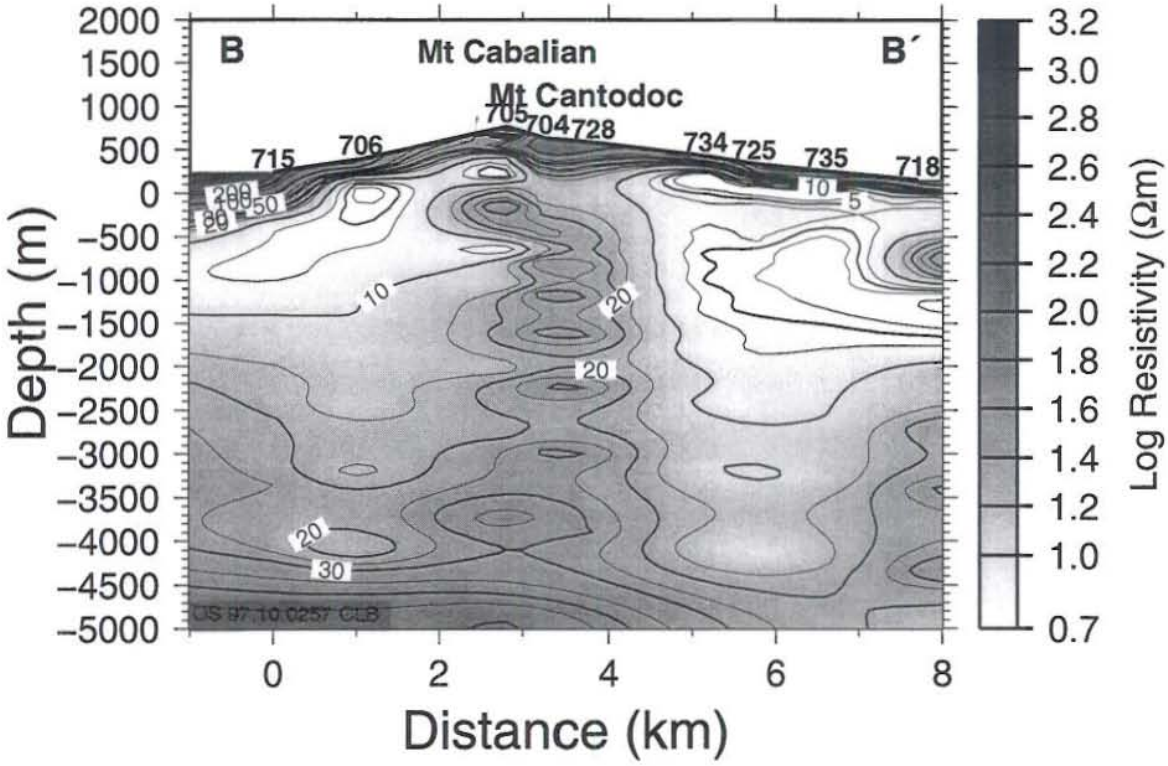

FIGURE 15: 1-D Occam model along cross-section B-B', contour interval is 0.1 log resistivity in Ωm

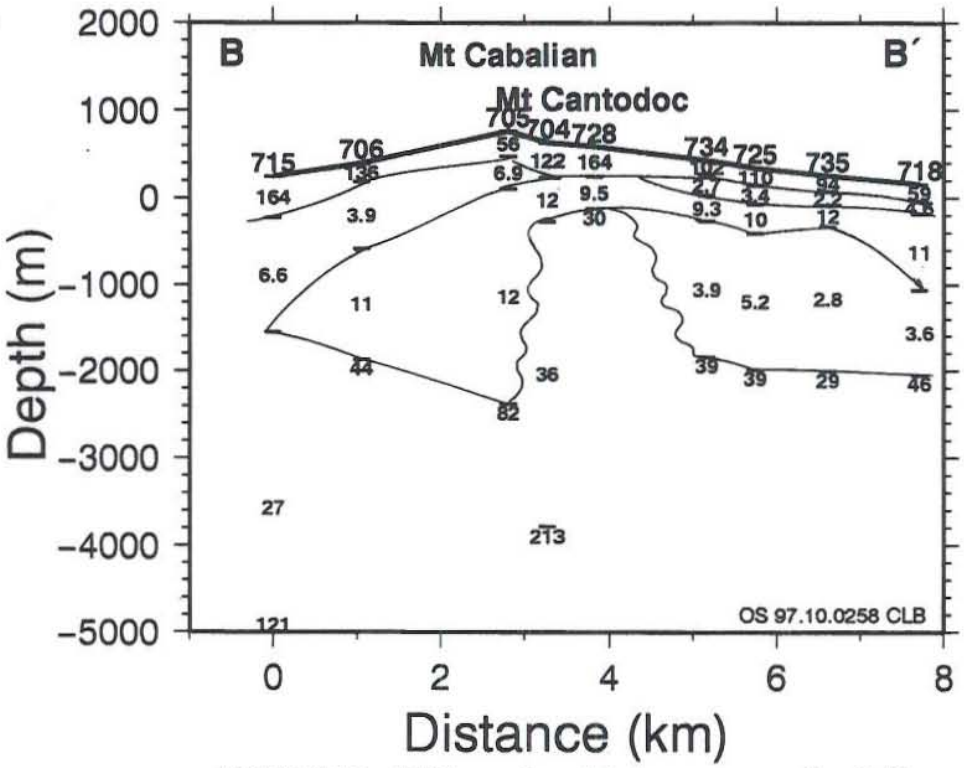

FIGURE 16: 1-D layered model along cross-section B-B', contour interval is 0.1 log resistivity in Ωm

ACKNOWLEDGEMENTS

First and foremost, I wish to thank Dr. Ingvar B. Fridleifsson and Mr. Lúdvík S. Georgsson for giving me the opportunity to participate in this Geothermal Training Programme. I also would like to express my gratitude to Dr. Hjálmar Eysteinsson, my adviser, for sharing his expertise in MT. Thanks are also due to the UNU lecturers for unselfishly teaching us about the other aspects of geothermal energy. My appreciation also goes to Mrs. Gudrún Bjarnadóttir and the other UNU fellows, for making my stay in Iceland as comfortable as possible. Lastly, I also would like to extend my sincere gratitude for the support given to me by my colleagues at PNOC-EDC.

REFERENCES

Catane, J.P.L., and Apuada, N.A., 1996: A gravity investigation of the Southern Leyte geothermal project. *Proceedings from the 18th PNOC-EDC annual geothermal conference, PNOC, Manila*, 288-295.

Constable, S.C., Parker, R.L., Constable, C.G., 1987: Occam's inversion: A practical algorithm for generating smooth models from electromagnetic sounding data. *Geophysics, 52-3,* 289-300.

Datuin, R.T., 1982: An insight on Quaternary volcanoes and volcanic rocks of the Philippines. *J. Geol. Soc. of Philippines, 36-1,* 1-11.

Gough, D.I. and Ingham, M.R., 1983: Interpretation methods for magnetometer arrays. *Reviews of Geophysics and Space Physics, 21-4,* 805-827.

Graham, G.B., 1991: *Overview of Phoenix V-5 MT receiver.* Phoenix Inc., USA, 8 pp.

Leynes, R.D., Bayon, F.E.B. and Camit, G.R.A.., 1996: The geology and geochemistry of the Southern Leyte geothermal project. *Proceedings from the 18th PNOC-EDC annual geothermal conference, PNOC, Manila,* 13-21.

Los Baños, C.E.F., 1997: *Appendix to the report: 1-D interpretation of magnetotelluric data from the Southern Leyte geothermal project, Philippines.* UNU G.T.P., report 10 appendix, 122 pp.

Patra, H.P. and Mallick, K. 1980: *Geosounding principles 2. Time-varying geoelectric soundings.* Elsevier Scientific Publishing Company, Amsterdam, 419 pp.

Swift Jr., C.M., 1967: A *magnetotelluric investigation of an electrical conductivity anomaly in the southwestern United States.* Ph. D. thesis, Massachusetts Institute of Technology, USA.

Tebar, H.J., Pagado, E.S., Villarosa, H.G.A., Buenviaje, M.M., Vergara, M.C., Maneja, F.C., Catane, J.P.L., and Herras, E.B., 1989. *Geoscientific exploration and evaluation of the Mt. Cabalian geothermal prospect, Southern Leyte.* PNOC EDC, Philippines, internal report, 77 pp.